Development of the acidity of zirconia-supported niobia catalysts

Thomas Onfroy[a], Guillaume Clet[a], Saeed B. Bukallah[b], David M. Hercules[b], and Marwan Houalla[a]*

[a]*Laboratoire de Catalyse et Spectrochimie (UMR CNRS 6506), ISMRA-Université de Caen, 6 Bd. du Maréchal Juin, 14050 Caen (cedex), France*

[b]*Department of Chemistry, Vanderbilt University, Nashville, TN, 37250, USA*

Received 10 February 2003; accepted 11 April 2003

A series of NbO_x/ZrO_2 catalysts containing up to 2.67 wt% Nb (ca. 80% nominal surface coverage) was prepared by incipient wetness impregnation from niobium oxalate and oxalic acid solution. The structure of the catalysts was monitored by X-ray diffraction and Raman spectroscopy. The results indicated the presence of a surface Nb phase. No evidence for the formation of crystalline Nb_2O_5 species was found. The development of the acidity as a function of Nb loading was monitored by adsorption of a basic probe molecule followed by infrared spectroscopy. The results indicated the appearance of Brönsted acid sites for a threshold of Nb loading. The abundance of Brönsted acid sites correlated well with the isopropanol dehydration activity. The overall behavior was very similar to that reported earlier for the WO_x/ZrO_2 system.

KEY WORDS: niobium oxide; zirconia; niobia zirconia catalysts; acidity; isopropanol dehydration; 2,6-dimethylpyridine adsorption; FT-IR.

1. Introduction

Supported tungsten and niobium oxides catalyze a wide variety of reactions [1–8]. For a number of these reactions, the catalytic performance is determined by the acidity of the surface species [9,10]. It is thus of interest to examine, for a given support, the development of the acidity as a function of the type and loading of the supported phase [11–14]. In a previous study, the evolution of the acidity of WO_x/ZrO_2 has been examined. The results indicated the appearance of Brönsted acidity for a threshold of W loading. The abundance of Brönsted acid sites correlated well with the isopropanol dehydration activity [15]. The purpose of the present work is to extend our investigation to include the related NbO_x/ZrO_2 system. Thus, a series of NbO_x/ZrO_2 catalysts was prepared by incipient wetness impregnation from niobium oxalate and oxalic acid solution. Niobium surface species were monitored by Raman spectroscopy. The number, the strength and the type of acidity were characterized by adsorption of basic probe molecules followed by IR spectroscopy. Isopropanol decomposition was used as test reaction to assay the acidity of the solids and to seek a correlation between acidity and catalytic performance.

2. Experimental

2.1. NbO_x/ZrO_2 catalysts synthesis

Degussa ZrO_2 (pore volume $\approx 0.4\,cm^3/g$, BET surface area $= 36\,m^2/g$) was mixed with deionized water, dried at 393 K for 24 h and calcined in air at 873 K for 24 h. Niobium deposition was carried out by incipient wetness impregnation, with a niobium oxalate/oxalic acid (7 wt% niobium oxalate) aqueous solution. The impregnated catalysts were then dried at 393 K for 16 h and calcined in air at 723 K for 16 h. Five different catalysts were prepared with Nb loadings ranging from 0.35 to 2.67 wt% Nb.

Samples will be designated as Zr Nby where y refers to the surface density in Nb atom/nm^2. The surface coverage was calculated by assuming that each Nb_2O_5 occupies an area of $0.32\,nm^2$ on the basis of the structure of crystalline Nb_2O_5 [16]. The main characteristics of the catalysts are reported in table 1.

2.2. Raman spectroscopy

Raman spectra were recorded with a Jobin-Yvon Dilor-LabRam spectrometer between 100 and $1100\,cm^{-1}$ (resolution: $2.6\,cm^{-1}$). The instrument was equipped with a He–Ne laser source (633 nm) and a CCD detector cooled by air. Samples were analyzed in a powder form and under ambient conditions without any pre-treatment.

Raman spectra were used to measure the relative amount of monoclinic and tetragonal zirconia, to detect the eventual presence of amorphous and crystalline Nb_2O_5 and to monitor the formation and the evolution of Nb surface species. The percentage of the different phases of zirconia was determined from the intensity of the monoclinic bands at 178 and $189\,cm^{-1}$ and the tetragonal band at $148\,cm^{-1}$. The monoclinic fraction

* To whom correspondence should be addressed.

1011-372X/03/0700–0015/0

Table 1
Characteristics of the solids

Catalysts	Zr Nb0	Zr Nb0.6	Zr Nb1.2	Zr Nb2.5	Zr Nb3.6	Zr Nb4.8
Nb_2O_5 content (wt%)	0.00	0.50	0.99	1.96	2.89	3.82
Nb content (wt%)	0.00	0.35	0.69	1.37	2.02	2.67
Surface density (at. Nb/nm^2)	0.0	0.6	1.2	2.5	3.6	4.8
Nominal coverage (%)	0	10	20	40	60	80

(C_m) can be determined from equation (1):

$$C_m = \frac{\frac{1}{2}(\mathrm{Im}(178) + \mathrm{Im}(189))}{k^*\mathrm{It}(148) + \frac{1}{2}(\mathrm{Im}(178) + \mathrm{Im}(189))} \quad (1)$$

where k is a correction factor for the difference of scattering cross section between monoclinic and tetragonal Raman bands [17].

2.3. Infrared spectroscopy

Infrared (IR) spectra were recorded with a Nicolet 710 FT-IR spectrometer (resolution: 4 cm^{-1}). Samples were pressed into discs ($\approx$10 mg/cm^2) and activated in vacuum at 723 K for 1 h. This was followed by a treatment in O_2 ($P_{equilibrium}$ = 13.3 kPa) for 1 h, and finally evacuated for 1 h at 723 K.

The acidic properties (type and abundance) of the samples were monitored by the use of two basic probe molecules (pyridine and 2,6-dimethylpyridine). Pyridine or 2,6-dimethylpyridine (Lutidine) were introduced at R.T. (P = 133 Pa) followed by thermal desorption from 373 to 573 K.

2.4. Catalytic activity

The isopropanol decomposition activity measurements were carried out in a fixed-bed flow reactor. A mass of ca. 40 mg of sample was pre-treated at 723 K for 1 h in 10% O_2/He (ca. 60 mL min^{-1}). The reactor was cooled to the reaction temperature and the system was purged by flowing ultra high purity (UHP) N_2 (ca. 60 mL min^{-1}) for 45 min. The reaction was performed at 473 K and at atmospheric pressure with N_2 (ca. 60 mL min^{-1}) as carrier gas and a partial pressure of isopropanol $P_{isopropanol}$ = 1.23 kPa. Reactants and products were analyzed with an on-line G.C. (Perkin-Elmer Sigma 200) equipped with a capillary column (Porapak-T) and an FID detector. The rate of propene formation was calculated from equation (2).

$$r = \frac{F_0}{W} \times \frac{C}{100} \quad (2)$$

where r is the rate of propene formation in mol h^{-1} g^{-1}, F_0 is the propan-2-ol molar flux in mol h^{-1}, W the mass of catalyst and C is the % conversion to propene.

3. Results

3.1. Raman spectroscopy

Figure 1 shows the Raman spectra of ZrO_2 and NbO_x/ZrO_2 catalysts, between 140 and 1100 cm^{-1}. The Raman spectrum of the zirconia support indicates the presence of two different crystalline forms: monoclinic with characteristic peaks at 176 and 188 cm^{-1}, and tetragonal with peaks at 144 and 263 cm^{-1} [18,19]. The monoclinic fraction of the support accounted for ca. 90% of the crystalline phases and was little affected by Nb addition. These results were consistent with XRD data. In the 800–1100 cm^{-1} region, the Raman spectra of NbO_x/ZrO_2 catalysts show a weak and broad band at 875 cm^{-1} which shifts to 920 cm^{-1} with increasing Nb loading. This band was previously attributed to the surface Nb phase [20]. The Raman spectrum of amorphous Nb_2O_5 (also called *niobic acid*) exhibits a band at, approximately, 650 cm^{-1} [16]. This band was not observed in our Raman spectra, suggesting that no significant formation of niobic acid occurs for the loadings examined in the present study. However, because of the partial overlap between the peak characteristic of niobic acid and that for the zirconia support at 635 cm^{-1}, the presence of niobic acid cannot be ruled out.

3.2. Infrared spectroscopy

3.2.1. Hydroxyl region

Figure 2 shows the infrared spectra for representative catalysts in the hydroxyl region (between 3900 and 3400 cm^{-1}). The infrared spectrum of the ZrO_2 support

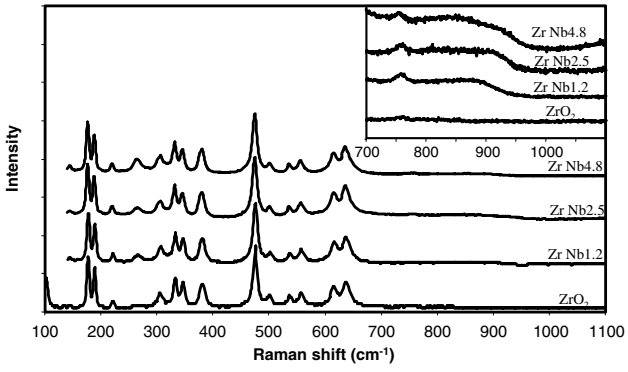

Figure 1. Raman spectra of Nb/ZrO_2 catalysts between 100 and 1100 cm^{-1}.

shows two peaks at 3777 cm^{-1} and 3676 cm^{-1}, attributed to isolated hydroxyls (type I) and bridged hydroxyls (type II) respectively [21,22]. Spectra of Nb/ZrO_2 indicate a preferential consumption of the more basic hydroxyl groups (peak at 3777 cm^{-1}), followed by a decrease in the intensity of the more acidic OH (peak at 3676 cm^{-1}) for higher Nb content. Figure 2 also shows that Nb addition leads to the appearance of a new band located at 3730 cm^{-1}, which increases in intensity and shifts to lower wave numbers with increasing Nb content.

3.2.2. Pyridine adsorption

Figure 3 shows the infrared spectra of adsorbed pyridine at 423 K between 1700 and 1400 cm^{-1}. The support and supported catalysts exhibit four peaks at 1608, 1575, 1488 and 1447 cm^{-1}, which can be attributed to pyridine coordinatively bound to Lewis acid sites. By increasing the Nb loading from 0 to 4.8 at./nm^2 the band at 1608 cm^{-1} shifts to 1611 cm^{-1}. A close inspection of the spectrum of Zr Nb4.8 indicates the presence of a very weak and broad band at ca. 1540 cm^{-1}, which could be associated with pyridine adsorbed on Brönsted acid sites to form pyridinium ions.

3.2.3. Lutidine adsorption

Pyridine adsorption results suggested the presence of Brönsted acidity for high Nb content. Brönsted acidity may also be present for lower Nb loading but may not be sufficiently strong to protonate pyridine. Lutidine (2,6-dimethylpyridine), which is more basic than pyridine, is a very sensitive probe molecule to detect relatively weak Brönsted acidity [23,24]. Figure 4 shows the infrared spectra of adsorbed Lutidine at

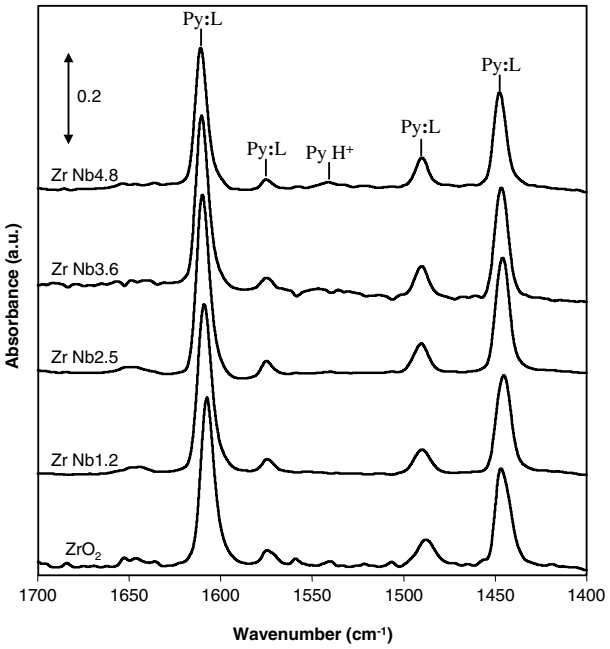

Figure 3. FTIR spectra of Nb/ZrO_2 catalysts after pyridine desorption at 423 K.

423 K between 1700 and 1590 cm^{-1}. The peak at ca. 1610 cm^{-1} can be attributed to lutidine coordinatively bound to Lewis sites. The doublet at ca. 1650 and 1630 cm^{-1} is associated with lutidine adsorbed on Brönsted acid sites to form lutidinium ions. Pure zirconia and catalysts up to 0.6 at. Nb/nm^2 did not exhibit any significant Brönsted acidity. At higher loading, Nb deposition brings about the formation of Brönsted acid sites. Figure 5 shows the evolution of the lutidinium peak as a function of Nb loading following desorption at 423 and 523 K. After desorption at 423 K,

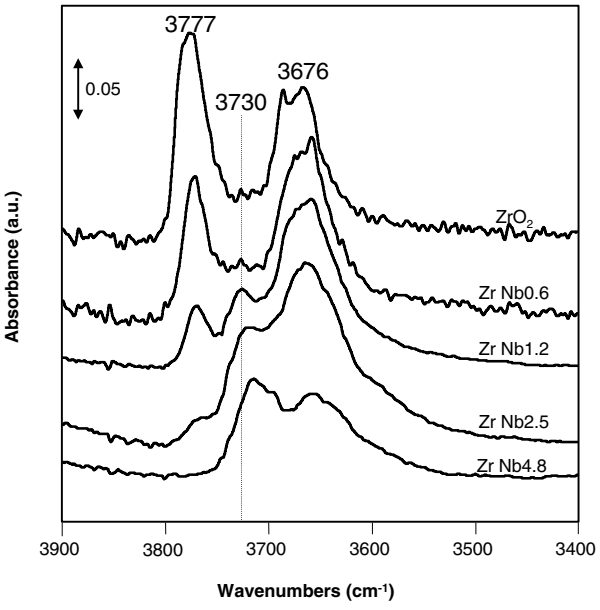

Figure 2. FTIR spectra of Nb/ZrO_2 catalysts in the hydroxyl region.

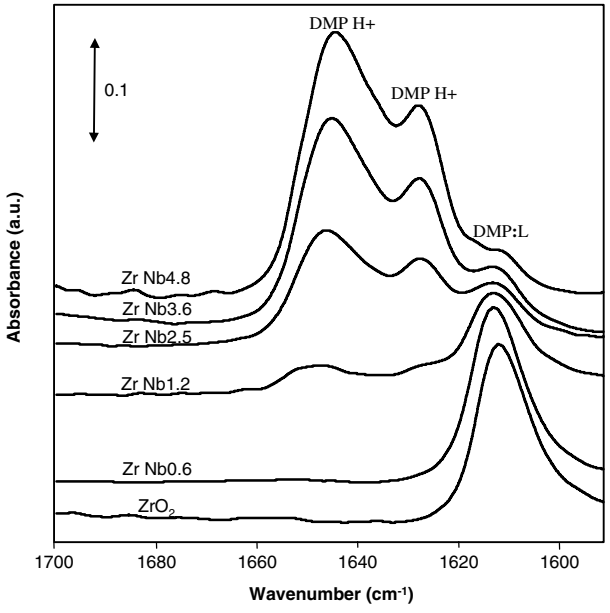

Figure 4. FTIR spectra of Nb/ZrO_2 catalysts after lutidine desorption at 423 K.

Brönsted acid sites were detected for loadings higher than 0.9 at. Nb/nm^2. Following desorption at 523 K, only solids containing more than 1.7 at. Nb/nm^2 exhibit Brönsted acidity sufficiently strong to retain lutidine. The abundance of these sites linearly increases with increasing Nb content.

3.3. Catalytic activity

Decomposition of isopropanol is a well-established test to evaluate the acidity of a solid. Dehydration to propene is known to occur on acidic catalysts [15,25,26], and dehydrogenation to acetone seems to occur on solids that have redox properties. Under our experimental conditions, the zirconia support was found to give a very low rate of propene formation (6.8×10^{-5} mol h^{-1} g^{-1}). The NbO_x/Zro_2 catalysts used in this study did not exhibit any dehydrogenation activity. Figure 6 shows the conversion of isopropanol as a function of Nb loading, after subtraction of the contribution of the zirconia support. The plot shows two distinct regions. Catalysts with Nb loadings less than 1.2 at./nm^2 exhibit little or no activity. As the Nb loading was increased from 2.5 to 4.8 at./nm^2 the rate of propene formation increased sharply from 0.85×10^{-3} to 2.86×10^{-3} mol h^{-1} g^{-1}.

4. Discussion

4.1. Development of the acidity of NbO_x/ZrO_2 catalysts

The acidic properties of niobium oxides supported on silica, alumina, magnesia, titania and zirconia have been examined by Datka *et al.* [14]. The evolution of Lewis and Brönsted acid sites was monitored by adsorption of pyridine followed by IR spectroscopy. Lewis acidity was found for all systems, whereas significant Brönsted acidity was only developed for the Nb/Al_2O_3 catalysts. In the latter case, Brönsted acid sites were detected after a critical Nb loading. Similar behavior was observed, in the present study, for the Nb/ZrO_2 system. This is at variance with the results of Datka *et al.* [14] where no appreciable Brönsted acidity was measured for the Nb/ZrO_2 solids. The apparent discrepancy can be readily explained if one takes into consideration the more basic character of the lutidine molecule used in the present study. This will allow the detection of weaker Brönsted acid sites that cannot protonate pyridine. The observed behavior of the Nb/ZrO_2 is similar to that reported for the W/ZrO_2 where Brönsted acidity was also detected after a threshold of *W* loading [4,12,15].

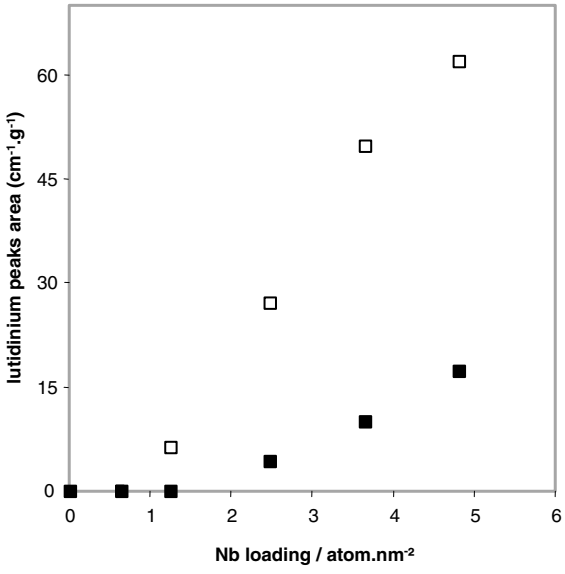

Figure 5. Evolution of the lutidinium peak area after desorption at 423 K (□) and 523 K (■).

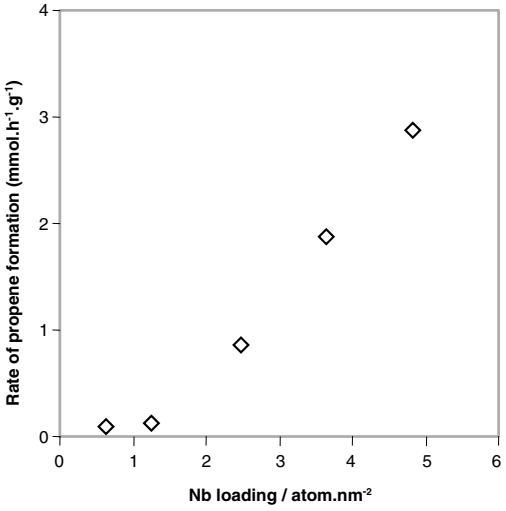

Figure 6. Activity of Nb/ZrO_2 catalysts for propan-2-ol dehydration at 473 K.

Infrared results also indicated the formation, on increasing Nb loading, of a new hydroxyl band located at ca. 3730 cm^{-1}. Based on Pyridine adsorption data, this peak was attributed by Burcham *et al.* [27] to weakly acidic (or non-acidic) Nb-OH or bridged Zr-OH-Nb species.

Figure 7 shows the variation of the catalytic activity and the abundance of Brönsted acid sites determined from lutidine adsorption experiments following desorption at 523 K, as a function of Nb content. One can clearly see that a direct relationship exists between isopropanol conversion and the abundance of Brönsted acid sites. The Brönsted acid sites of the zirconia support and the low loading catalysts are either inactive or weakly active for isopropanol decomposition. The onset of significant activity coincides with the appearance of Brönsted acidity and evolves in a parallel fashion with increasing Nb content. Thus, the decomposition of propan-2-ol on NbO_x/Zro_2 catalysts appears to be directly related to the presence and abundance of

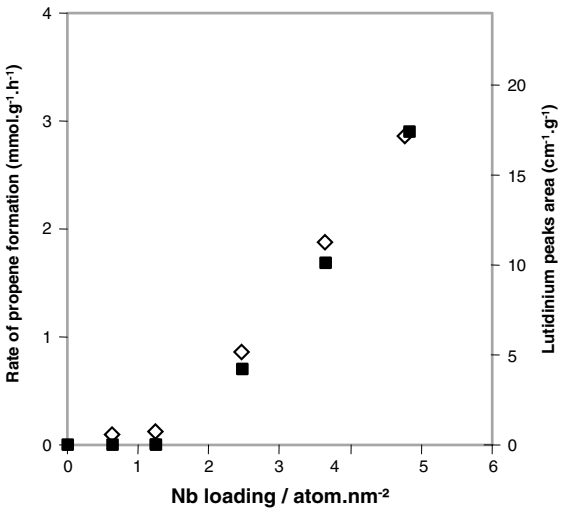

Figure 7. Correlation between Brönsted acidity (■) and catalytic activity for propan-2-ol dehydration (◇) over Nb/ZrO_2 catalysts.

Brönsted acid sites as monitored by Lutidine adsorption. These findings are in accord with those reported in our previous study of WO_x/ZrO_2 system [15].

4.2. *Molecular structure of Nb species; nature of active site*

Raman study of the NbO_x/ZrO_2 samples indicated that for nominal coverage up to 80%, the Nb phase is present essentially as a surface species. No clear indications for the presence of bulk niobic acid (band at 660 cm^{-1}) were found. Similarly, no bands that could be assigned to crystalline Nb_2O_5 [16] were detected. The surface species is evidenced, on our catalysts, by a weak and broad band at 875 cm^{-1}, which shifts to 920 cm^{-1} with increasing Nb loading. The molecular structure of NbO_x/ZrO_2 catalysts following *in situ* dehydration has been examined by Wachs and coworkers [27]. Their results indicated the presence of isolated monomeric Nb species for low Nb loadings (ca. 20% coverage) and polymeric Nb species for high Nb content (near monolayer coverage). By comparing the reported structure of Nb species with the observed isopropanol decomposition activity and the abundance of Brönsted acid sites, one can infer that monomeric species do not exhibit Brönsted acidity and thus are essentially inactive. The catalytic activity appears to be associated with polymeric Nb species. As previously noted in the case of the WO_x/ZrO_2 system, the development of Brönsted acidity with increasing Nb loading may be explained by proton stabilization by delocalization of the negative charge over the Nb cluster.

5. Conclusions

The development of the acidity series of NbO_x/ZrO_2 catalysts containing up to 2.67 wt% Nb (ca. 80% nominal surface coverage) as a function of Nb loading was monitored by adsorption of a basic probe molecule followed by infrared spectroscopy. The results indicated the appearance of Brönsted acid sites for a threshold of Nb loading. The abundance of Brönsted acid sites correlated well with the isopropanol dehydration activity. The overall behavior was very similar to that reported earlier for the WO_x/ZrO_2 system.

References

[1] J.C. Mol and J.A. Moulijn, in *Catalysis-Science and Technology*, eds. J.R. Anderson and M. Boudard (Springer, Berlin, 1987).
[2] F. Hilbrig, H. Schmelz and H. Knözinger, in *Proc. 10th International Congress on Catalysis*, eds. L. Guczi, F. Solymosi and P. Tetényi (Elsevier, Amsterdam, 1993) p. 1351.
[3] A. Gutiérrez-Alejandre, P. Castillo, J. Ramirez, G. Ramis and G. Busca, Appl. Catal., A 216 (2001) 181.
[4] J.G. Santiesteban, J.C. Vartuli, S. Han, R.D. Bastian and C.D. Chang, J. Catal. 168 (1997) 431.
[5] I. Nowak and M. Ziolek, Chem. Rev. 99 (1999) 3603.
[6] K. Tanabe and S. Okazaki, Appl. Catal., A 133 (1995) 191.
[7] J.M. Jehng and I.E. Wachs, Catal. Today 16 (1993) 417.
[8] I.E. Wachs, J.M. Jehng, G. Deo, H. Hu and N. Arora, Catal. Today 28 (1996) 199.
[9] R.D. Wilson, D.G. Barton, C.D. Baertsch and E. Iglesia, J. Catal. 194 (2000) 175.
[10] R.Y. Weng and J.F. Lee, Appl. Catal., A 105 (1993) 41.K.
[11] M. Scheithauer, R.K. Grasselli and H. Knözinger, Langmuir 14 (1998) 3019.
[12] D.G. Barton, M. Shtein, R.D. Wilson, S.L. Soled and E. Iglesia, J. Phys. Chem. B 103 (1999) 630.
[13] I.E. Wachs, Catal. Today 27 (1996) 437.
[14] J. Datka, A.M. Turek, J.M. Jehng and I.E. Wachs, J. Catal. 135 (1992) 186.
[15] T. Onfroy, G. Clet and M. Houalla, Chem. Commun. 15 (2001) 1378.
[16] R.M. Pittman and A.T. Bell, J. Phys. Chem. 97 (1993) 12178.
[17] G. Katagiri, H. Ishida and A. Ishitani, in *Science and Technology of Zirconia III*, eds. S. Somiya, N. Yamamoto and H. Yanagida (American Ceramic Society, Westerville, USA, 1998) p. 537.
[18] B.K. Kim, J.W. Hahn and K.R. Han, J. Mater. Sci. Lett. 16 (1997) 669.
[19] B. Zhao, X. Xu, J. Gao, Q. Fu and Y. Tang, J. Raman Spectrosc. 27 (1996) 549.
[20] J.M. Jehng and I.E. Wachs, J. Mol. Catal. 67 (1991) 369.
[21] T. Yamaguchi, Y. Nakano and K. Tanabe, Bull. Chem. Soc. Jpn. 51 (1978) 2482.
[22] M. Bensitel, V. Moravek, J. Lamotte, O. Saur and J.C. Lavalley, Spectrochim. Acta 43A (1987) 1487.
[23] P.A. Jacobs and C.F. Heylen, J. Catal. 34 (1974) 267.
[24] A. Corma, C. Rodellas and V. Fornes, J. Catal. 88 (1984) 374.
[25] C. Lahousse, F. Mauge, J. Bachelier and J.C. Lavalley, J. Chem. Soc., Faraday Trans. 91 (1995) 2907.
[26] D. Haffad, A. Chambellan and J.C. Lavalley, J. Mol. Catal., A 168 (2001) 153.
[27] L.J. Burcham, J. Datka and I.E. Wachs, J. Phys. Chem. B 103 (1999) 6015.